

Spatially-Directed Oxidation of Gold Nanoparticles by Au(III)–CTAB Complexes

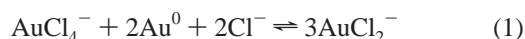
Jessica Rodríguez-Fernández,[†] Jorge Pérez-Juste,[†] Paul Mulvaney,[‡] and Luis M. Liz-Marzán^{*,†}*Departamento de Química Física, Universidade de Vigo, 36310, Vigo, Spain, and Chemistry School, University of Melbourne, Parkville 3010, VIC., Australia**Received: May 13, 2005; In Final Form: June 15, 2005*

Gold nanoparticles are readily oxidized by Au(III) in the presence of cetyl-trimethylammonium bromide (CTAB). Oxidation occurs preferentially at surface sites with higher curvature. Conversely, oxidation with cyanide ions in the absence of CTAB leads to uniform oxidation over the whole surface. Examples of the spatially directed oxidation are provided using large, irregular spheres, nanocubes, and nanorods. We conclude that the mechanism of oxidation depends on whether the oxidant is attached to CTAB micelles. It is postulated that the CTAB micelles approach the nanoparticles preferentially at the tips, leading to spatially directed oxidation.

Introduction

The ability to tailor the shape of inorganic nanocrystals is a fundamental challenge to materials scientists. Though a number of empirical procedures have recently been developed to prepare monodisperse metal nanorods,^{1–5} multipods,⁶ nanoprisms,^{7–10} nanocubes,^{11,12} nanotetrahedra,^{12,13} or nanodisks,^{14,15} there is still relatively little understood about the mechanisms that determine crystal habit and morphology.^{5,16,17} In particular, the growth of gold nanorods induced by the presence of the cationic surfactant cetyl-trimethylammonium bromide (CTAB), initially devised by Murphy and co-workers,¹⁸ has become very popular and various mechanisms have been proposed to explain it. Such mechanisms primarily focus on selective blocking of certain crystallographic faces or anisotropic surface properties that control the approach of metal ions from solution. We have recently shown that the AuCl_4^- ions are quantitatively bound to CTAB micelles. These micelles are electrostatically repelled from the CTAB capped gold rods. However, the numerical solutions revealed that the flux of micelles (and gold ions) is higher at the tips.⁵ This suggests that crystal growth can be manipulated and spatially controlled by CTAB if the active solution species that deposits onto the growing particle surface is adsorbed to the CTAB micelles. Conversely, in its absence corrosion should be homogeneous over the particle surface.

We report here on the dissolution of gold rods by AuCl_4^- via reaction 1



which only takes place in the presence of CTAB because of a change in the reduction potential of AuCl_4^- upon complexation (see discussion below), and leads to gradual oxidation of Au nanoparticles (irrespective of particle shape). Careful analysis

of this reaction shows that it occurs preferentially at nanoparticle surface sites with higher radius of curvature, and provides an elegant procedure for the narrowing of the nanoparticle size and shape distribution. Actually, this process has been observed by Halas and co-workers¹⁹ during reshaping experiments on Au nanoshells driven by CTAB, though Au oxidation was not reported.

Experimental Details

Tetrachloroauric acid ($\text{HAuCl}_4 \cdot 3\text{H}_2\text{O}$), sodium citrate, cetyl-trimethylammonium bromide (CTAB), benzyldimethylammonium chloride (BDAC), ascorbic acid, sodium borohydride (NaBH_4), and AgNO_3 were purchased from Aldrich. Milli-Q water with a resistivity higher than 18.2 $\text{M}\Omega \text{ cm}$ was used in all of the preparations.

Au spherical particles (15 nm diameter) were synthesized using the citrate reduction method developed by Turkevich.²⁰ Spheroidal particles with mean diameters between 70 and 90 nm were prepared according to the seed mediated method proposed by Natan and co-workers,²¹ in which 3 nm seeds (prepared by reduction of HAuCl_4 with NaBH_4 using sodium citrate as a stabilizer) are grown by boiling them in a solution of HAuCl_4 and sodium citrate. For the oxidation experiments, citrate was replaced with CTAB 0.05M upon addition of a suitable volume of a concentrated surfactant solution. Au nanorods were prepared through a modification of the seeding method published by Nikoobakht and El-Sayed,⁴ growing CTAB stabilized Au nanoparticle seeds (<3 nm) by reduction of HAuCl_4 with ascorbic acid, in the presence of a BDAC/CTAB mixture and a small amount of AgNO_3 . The aspect ratio is controlled by the amount of seed solution added. Prior to the oxidation experiments, the Au nanorods were centrifuged, the supernatant discarded, and the nanorods redispersed in a 0.05 M CTAB solution.

Results and Discussion

A. Stoichiometry and Reaction Rate. The redox chemistry of gold in aqueous solutions at room temperature is dominated

* To whom correspondence should be addressed. E-mail: lmarzan@uvigo.es.

[†] Universidade de Vigo.

[‡] University of Melbourne.

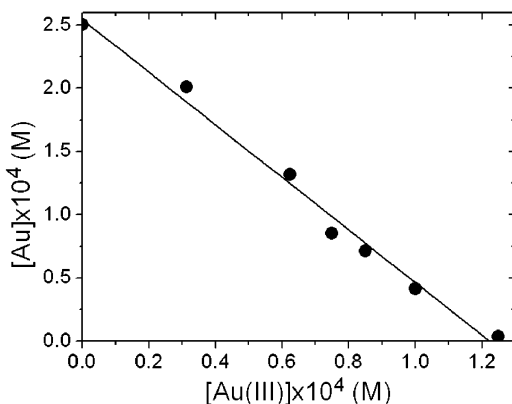
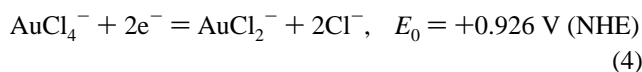
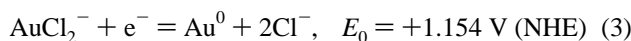
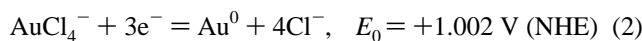


Figure 1. Variation in $[\text{Au}^0]$ as Au(III) is added to a gold colloid (initially 2.50×10^{-4} M), in the presence of CTAB (0.05 M). The straight line is a linear fit to the data, which yields a slope of -2.1 ± 0.1 . Complete oxidation is observed when $[\text{Au(III)}] = 1.25 \times 10^{-4}$ M.

by the following redox reactions:



It is evident that the reduction of gold (III) to gold (I) and gold (I) to Au^0 are both very electropositive reactions. From these reduction potentials, the comproportionation of AuCl_2^- via reaction 1 is very unfavorable.



In typical colloid solutions containing 0.25 mM gold metal as colloid particles and 0.75 mM chloride ions from the preparation, the addition of 0.125 mM HAuCl_4 would lead to the formation of just $1.1 \mu\text{M}$ of AuCl_2^- . Hence the reaction of gold chloride with gold metal is virtually negligible. However, the binding of AuCl_4^- to the CTAB micelles drastically alters the value of the equilibrium constant for the comproportionation and enables gold particles to be quantitatively dissolved by the gold salt. Strictly, one should consider that chloride ions from AuCl_4^- will (at least partially) exchange with bromide ions from CTAB. This will affect the value of the redox potentials and the equilibrium constant, since the bromide concentration is much higher. Details are provided in the Supporting Information.

This shift in the equilibrium constant is illustrated in Figure 1, which presents the changes in Au^0 concentration (estimated from the absorbance at 400 nm, which is assumed to have a size independent absorption coefficient) as the $\text{HAuCl}_4/\text{CTAB}$ mixture is added to the colloid. A linear fit to the data yields a slope of -2.1 ± 0.1 which confirms that two moles of Au^0 are consumed for each mole of Au(III) added, in accordance with reaction 1. Reaction 1 is basically stoichiometric (with a very high equilibrium constant), since a $\text{Au}^0:\text{Au}^{\text{III}}$ molar ratio of 1.0:0.5 is sufficient for complete oxidation of the Au^0 nanoparticles and a linear decrease in the metallic gold concentration is observed during titration with the $\text{HAuCl}_4/\text{CTAB}$ complex. From the absorbance we estimate there is less than $1 \mu\text{M}$ HAuCl_4 remaining after the addition of 0.125 mM HAuCl_4 . Hence the equilibrium constant for the comproportionation must be at least $K > (3.75 \times 10^{-4})^3 / [1 \times 10^{-6} \times (7.5 \times 10^{-4})^2] = 93.8$. Hence, the equilibrium constant is increased by at least

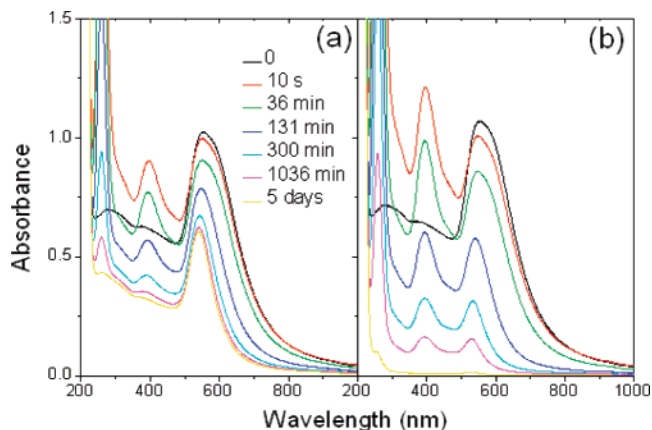


Figure 2. Time evolution of the UV-vis spectra during oxidation of Au nanoparticles in water before (0) and after addition of HAuCl_4 in the presence of CTAB 0.05 M. $\text{Au}:\text{Au}^{\text{III}}$ molar ratios are (a) 1:0.25 and (b) 1:0.5.

4.9×10^9 in the presence of the cationic surfactant. This shift is due to the strong binding of AuCl_2^- to the CTAB micelles. If this is attributed solely to the high binding constant of Au(I) to the cationic micelles, then the redox potential for reaction 3 is cathodically shifted by at least 0.6 V to a value of +0.4V NHE in the presence of CTAB.

B. Oxidation of Irregular Nanoparticles. One first demonstration that the reaction occurs preferentially at surface sites with a higher curvature is provided by the morphological changes observed during the oxidation of large nanoparticles with a marked ellipticity (deviation from spherical shape). These nanoparticles were prepared by growth of ca. 3 nm seeds (see the Experimental Section) by boiling them in a solution of HAuCl_4 and sodium citrate. The growth is rather fast and leads to nanoparticles with an average diameter of ≈ 70 nm and rather irregular shapes. If, after cooling, AuCl_4^- is added to these nanoparticles in the absence of CTAB, no changes in either the optical response (plasmon band position, shape, or intensity) or the morphology of the particles (characterized by TEM) are observed, but if both the nanoparticles and the Au salt are premixed with CTAB, then upon mixing there is a gradual change in the spectrum (see Figure 2). There is a systematic blue-shift of the absorption peak, a clear decrease in the peak intensity, a narrowing of the absorption band, and an increase in the symmetry of the band profile.²² Such spectral changes are consistent with the gradual oxidation of Au^0 since a decrease in particle size will lower the absorbance and cause a blue-shift, but the narrowing and increased symmetry of the surface plasmon absorption band also suggest that there is a progressive increase in monodispersity.²³

The evolution of the nanoparticle morphology during the reaction was monitored using TEM. Samples were obtained by adding different concentrations of HAuCl_4 to identical aliquots of the same starting colloid and allowing the reaction to proceed until the spectrum did not change. Examples of the TEM observations are shown in Figure 3. The corresponding size and shape distributions are provided as Supporting Information and are also summarized in Table 1. It is obvious from the micrographs, but especially from the histograms that not only does the size gradually decrease but the size distribution and the ellipticity (defined as the ratio between long and short axes) are both much narrower. Thus, it is clear that the reaction preferentially occurs at surface sites with a higher curvature, so that sharp protuberances gradually disappear and smoother surfaces are obtained. Since in general the larger particles in

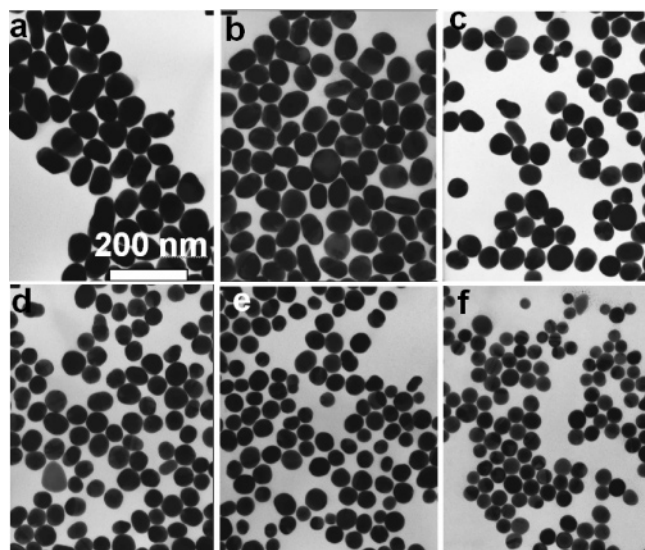


Figure 3. TEM micrographs of Au nanoparticles before (a) and after addition of HAuCl_4 with different $\text{Au}:\text{Au}^{\text{III}}$ molar ratios [1:0.125 (b), 1:0.25 (c), 1:0.30 (d), 1:0.34 (e), 1:0.4 (f)] in the presence of CTAB 0.05 M.

TABLE 1: Average Values of the Dimensions (Width and Length) and Ellipticity of Au Nanoparticles Oxidized with Varying Amounts of HAuCl_4

$[\text{Au}]:[\text{Au}^{\text{III}}]$	length (nm)	width (nm)	ellipticity (L/W)
1:0	96.3 ± 20.9	68.9 ± 13.2	1.40 ± 0.28
1:0.125	76.0 ± 10.0	57.5 ± 8.1	1.35 ± 0.29
1:0.25	62.4 ± 8.1	53.9 ± 7.1	1.16 ± 0.16
1:0.30	57.3 ± 6.7	50.0 ± 6.5	1.15 ± 0.15
1:0.34	51.5 ± 8.1	45.5 ± 7.3	1.13 ± 0.14
1:0.40	43.9 ± 6.6	40.9 ± 5.8	1.07 ± 0.05

the starting colloid were also those with a larger ellipticity, their size was further reduced and monodispersity is globally improved.

We have so far demonstrated that this reaction only takes place in the presence of CTAB, and since we are working above the cmc, CTAB forms micelles, which carry complexed AuCl_4^- ions. If the concentration of CTAB is lower than the cmc, precipitation of the AuCl_4^- ions complexed with CTAB monomers is observed, since its solubility constant is $K \sim 10^{-12}$.²⁴

Importantly, the different shaped gold nanoparticles expose different crystallographic facets to the solution at the protuberances. Since they all display the same surface smoothing during oxidation, we must conclude that the mechanism that leads to spatially directed oxidation of the particles is independent of the exact crystallographic facets present at the sharply curved points on the particle surface. Hence it is not determined by the specific binding of CTAB to particular facets, but is a consequence of the high local curvature. This suggests that both reduction of AuCl_4^- to form gold rods and the dissolution of the rods both take place at the rod termini. Micellization of the gold salt leads to preferred electron transfer at the tips and implies that the collision frequency of micelles with the gold rods is higher at the tips.

C. Oxidation in Binary Mixtures. The influence of particle size on the oxidation rate was studied by addition of $\text{AuCl}_4^-/\text{CTAB}$ solutions to both Au colloids with different particle size (15 and 60 nm) and binary mixtures of them. According to the model described in the previous section, there should be a higher flux of CTAB micelles to smaller particles (with a higher curvature) and these should therefore be preferentially oxidized.

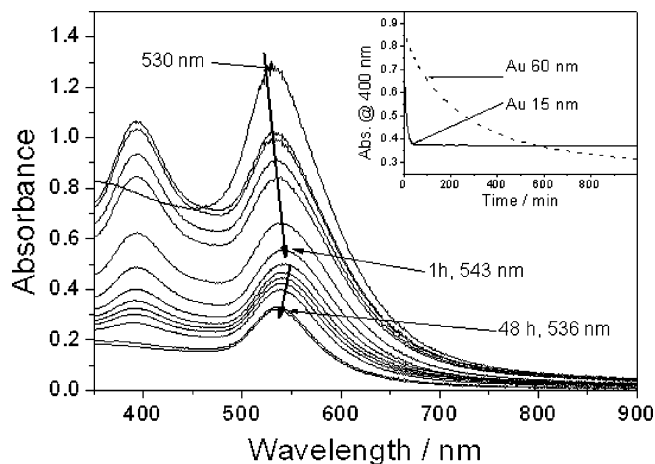


Figure 4. Spectral evolution of an equimolar mixture of large (60 nm) and small (15 nm) Au nanoparticles during oxidation with HAuCl_4 ($[\text{Au}]:[\text{Au}^{\text{III}}] = 1:0.39$) in the presence of CTAB 0.05 M. The inset shows the kinetic traces for separate oxidation of both colloids ($[\text{Au}]:[\text{Au}^{\text{III}}] = 1:0.25$). The absorption at 400 nm is due to the $\text{Au}(\text{III})$ –CTAB complex. It disappears during the course of the reaction.

The results obtained for the pure colloids are summarized in the inset of Figure 4, which shows the time evolution of the absorbance at 400 nm upon $\text{AuCl}_4^-/\text{CTAB}$ addition. At this wavelength, the absorption is mainly due to interband transitions (with some contribution from light scattering) and the absorption coefficient is roughly independent of particle size. From the plot, it is apparent that for smaller particle sizes, the decay rate is indeed faster.

During oxidation of binary mixtures, it is observed that the smaller nanoparticles dissolve first, and when they have been totally consumed, the larger ones are still almost unaffected. This has been observed both by TEM and by UV–vis spectroscopy. Although the SP bands of the two different populations within the sample are close to each other, the spectral evolution (Figure 4) is quite conclusive. Initially, the absorption band results from the sum of the contributions from both sizes. Once the oxidation starts (first hour) there is a red shift due to consumption of the smaller particles (smaller contribution at lower wavelengths), and thereafter, the band slowly blue-shifts because of the decrease in ellipticity as described above. These time scales also agree with those observed for oxidation of the separate colloids (inset). Additionally, TEM (Figure 5) shows that, during the oxidation of the mixture, the number of small particles decreases (smaller ones are oxidized first), whereas the bigger ones basically maintain their size while the smaller ones are not completely consumed. Upon oxidation in the mixture, the size of the larger particles changes from 67.0×51.6 nm down to 63.6×52.3 nm, while the same amount of HAuCl_4 leads, in the absence of small spheres, to a final size of 48.7×45.0 nm.

D. Oxidation of Au Nanorods. Nanorods provide an extreme case of curvature changes within a single nanoparticle, since they possess basically flat sides and highly curved tips. Thus, if the above reasoning is correct, oxidation of Au nanorods with $\text{Au}(\text{III})$ –CTAB complexes should lead to a progressive shortening of the rods with almost no change in the width. To provide a clear demonstration of this effect, we have chosen samples with relatively high aspect ratio (around 5). The synthesis was based on the procedure reported by Nikoobakht and El-Sayed,⁴ in which AgNO_3 is added to increase the yield of rods formed and a mixture of surfactants (CTAB and BDAC) is used to induce larger aspect ratios. The result is a mixture of mostly

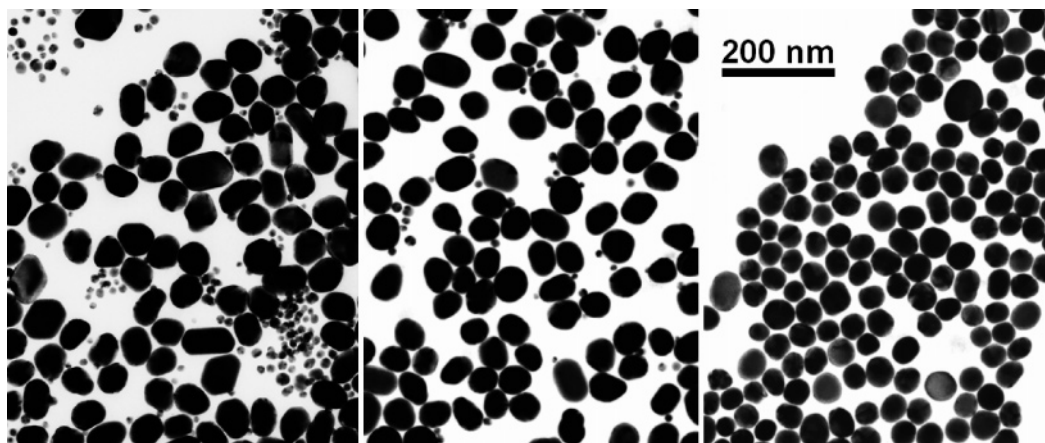


Figure 5. Representative TEM images of an equimolar mixture of large (60 nm) and small (15 nm) Au nanoparticles at various times (from left to right: 0, 1, 48 h) during oxidation with HAuCl_4 ($[\text{Au}]:[\text{Au}^{\text{III}}] = 1:0.39$) in the presence of CTAB 0.05 M.

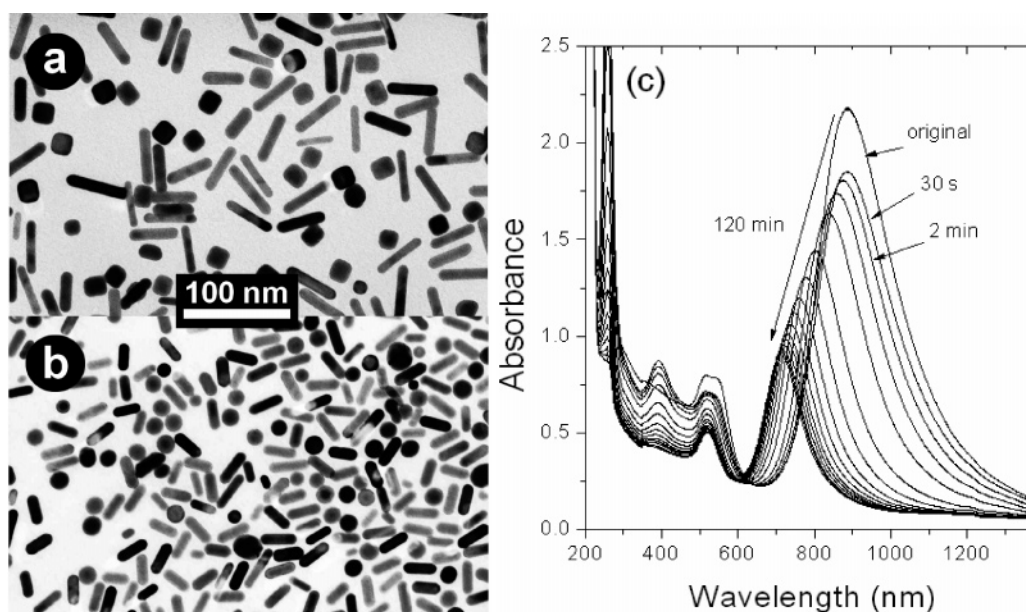


Figure 6. TEM micrographs of Au nanorods (a) before and (b) after oxidation with HAuCl_4 ($[\text{Au}]:[\text{Au}^{\text{III}}] = 1:0.25$) in the presence of CTAB 0.05 M. (c) UV-vis-NIR spectral evolution of Au nanorods shown in (a) during oxidation with HAuCl_4 in the presence of CTAB.

TABLE 2: Average Values of the Dimensions (Width and Length) and Aspect Ratio of Au Nanorods before and after Oxidation with HAuCl_4 -CTAB

	length (nm)	width (nm)	aspect ratio (L/W)
Au-CTAB before	48.3 ± 6.4	10.0 ± 1.7	4.97 ± 1.00
Au-CTAB after	28.9 ± 4.5	10.4 ± 1.4	2.80 ± 0.45

rods (68%) and cubes (32%), as shown in Figure 6a. When HAuCl_4 is added in the presence of CTAB, absorption spectroscopy (Figure 6c) reveals a gradual blue shift and decrease of the longitudinal surface plasmon band, indicating the expected decrease in aspect ratio, which is also confirmed by TEM (see Figure 6b and Table 2). TEM images also show that nanocubes present in the sample become more spherical after the oxidation. This is probably related to the extreme curvature associated with such acute tips. This cube-to-sphere conversion is also reflected in the UV-vis spectra, since the band at 545 nm (due to nanocubes) in the spectrum at time zero quickly merges with the absorption band, around 520 nm due to excitation of surface plasmons in spherical nanoparticles.

Related experiments were performed by Murphy and co-workers using cyanide as oxidant.²⁵ They have shown that in the presence of cyanide, short spheroids with sharp tips dissolve

preferentially from the tips, leading to lower aspect ratio nanorods and eventually to spheres. However, for longer nanorods, cyanide oxidation occurred at various spots along the side edges, with no intermediate shorter rods being formed, in sharp contrast to the results shown in Figure 6. In the experiments of Murphy and colleagues, excess CTAB was removed by centrifugation prior to the oxidation reaction, so it is clear that the interaction between the gold nanoparticle surface and CTAB micelles plays a fundamental role in the oxidation mechanism.

Conclusions

Au(III) can oxidize Au nanoparticles in the presence of CTAB. The redox reaction takes place between Au^0 and AuCl_4^- ions complexed with CTAB micelles, and because the CTAB concentration is above the cmc, the oxidant is confined to the positively charged micelles. Hence the spatially directed oxidation is attributed to the differences in the flux of micelles to highly curved and flat surfaces of the different gold nanoparticles. Use of such a reaction with irregular gold nanoparticles leads to a drastic decrease in surface roughness and ellipticity, along with particle size. In the case of nanorods, the

length is primarily affected, while the thickness remains almost constant during the reaction.

Acknowledgment. Financial support from the Spanish Ministerio de Educación y Ciencia/FEDER (Project MAT2004-02991) is gratefully acknowledged.

Supporting Information Available: Discussion on the effect of bromide ions on the equilibrium constant of eq 1 and TEM micrographs along with ellipticity, length and width histograms of Au nanoparticles before and after addition of H₂AuCl₄ with various Au:Au^{III} molar ratios. This material is available free of charge via the Internet at <http://pubs.acs.org>.

References and Notes

- (1) van der Zande, B. M. I.; Boehmer, M. R.; Fokkink, L. G. J.; Schoenenberger, C. J. *J. Phys. Chem. B* **1997**, *101*, 852.
- (2) Chang, S.-S.; Shih, C.-W.; Chen, C.-D.; Lai, W.-C.; Wang, C. R. *C. Langmuir* **1999**, *15*, 701.
- (3) Busbee, B. D.; Obare, S. O.; Murphy, C. J. *Adv. Mater.* **2003**, *15*, 414.
- (4) Nikoobakht, B.; El-Sayed, M. A. *Chem. Mater.* **2003**, *15*, 1957.
- (5) Pérez-Juste, J.; Liz-Marzán, L. M.; Carnie, S.; Chan, D. Y. C.; Mulvaney, P. *Adv. Funct. Mater.* **2004**, *14*, 571.
- (6) Chen, S.; Wang, Z. L.; Ballato, J.; Foulger, S. H.; Carroll, D. L. *J. Am. Chem. Soc.* **2003**, *125*, 16186.
- (7) Jin, R.; Cao, Y.; Mirkin, C. A.; Kelly, K. L.; Schatz, G. C.; Zheng, J. G. *Science* **2001**, *294*, 1901.
- (8) Pastoriza-Santos, I.; Liz-Marzán, L. M. *Nano Lett.* **2002**, *2*, 903.
- (9) Millstone, J. E.; Park, S.; Shuford, K. L.; Qin, L.; Schatz, G. C.; Mirkin, C. A. *J. Am. Chem. Soc.* **2005**, *127*, 5312.
- (10) Sun, Y.; Xia, Y. *Adv. Mater.* **2003**, *15*, 695.
- (11) Im, S. H.; Lee, Y. T.; Wiley, B.; Xia, Y. *Ang. Chem. Int. Ed.* **2005**, *44*, 2154.
- (12) Kim, F.; Connor, S.; Song, H.; Kuykendall, T.; Yang, P. *Ang. Chem. Int. Ed.* **2004**, *43*, 3673.
- (13) Wiley, B.; Herricks, T.; Sun, Y.; Xia, Y. *Nano Lett.* **2004**, *4*, 1733.
- (14) Maillard, M.; Giorgio, S.; Pileni, M.-P. *J. Phys. Chem. B* **2003**, *107*, 2466.
- (15) Maillard, M.; Huang, P.; Brus, L. *Nano Lett.* **2003**, *3*, 1611.
- (16) Jin, R.; Cao, Y. C.; Hao, E.; Metraux, G. S.; Schatz, G. C.; Mirkin, C. A. *Nature* **2003**, *425*, 487.
- (17) Giersig, M.; Pastoriza-Santos, I.; Liz-Marzán, L. M. *J. Mater. Chem.* **2004**, *14*, 607.
- (18) Jana, N. R.; Gearheart, L.; Murphy, C. J. *J. Phys. Chem. B* **2001**, *105*, 4065.
- (19) Aguirre, C. M.; Kaspar, T. R.; Radloff, C.; Halas, N. J. *Nano Lett.* **2003**, *3*, 1707.
- (20) Turkevich, J.; Stevenson, P. C.; Hillier, J. *Discuss. Faraday Soc.* **1951**, 55.
- (21) Brown, K. R.; Walter, D. G.; Natan, M. J. *Chem. Mater.* **2000**, *12*, 306.
- (22) Two additional absorption bands appear in the spectrum, which are related with the CTTS of AuCl₄⁻ (255 nm) and with the AuCl₄⁻-CTAB complex (393 nm). Both bands completely disappear upon complete reduction of Au(III) to Au(I).
- (23) Link, S.; El-Sayed, M. A. *J. Phys. Chem. B* **1999**, *103*, 8140.
- (24) Esumi, K.; Matsuhisa, K.; Torigoe, K. *Langmuir* **1995**, *11*, 3285.
- (25) Jana, N. R.; Gearheart, L.; Obare, S. O.; Murphy, C. J. *Langmuir* **2002**, *18*, 922.